Direction Modulation of Muscle Synergies in a Hand-Reaching Task

Sharon Israely, Gerry Leisman, *Senior Member, IEEE*, Chay Machluf, Tal Shnitzer, and Eli Carmeli

***Abstract*— Functional tasks of the upper extremity can be executed by a variety of muscular patterns, independent of the direction, speed and load of the task. This large number of degrees of freedom imposes a significant control burden on the CNS. Previous studies suggested that the human cortex synchronizes a discrete number of neural functional units within the brainstem and spinal cord, i.e. muscle synergies, by linearly combining them to execute a great repertoire of movements. Further exploring this control mechanism, we aim to study whether a single set of muscle synergies might be generalized to express movements in different directions. This was implemented by using a modified version of the non-negative matrix factorization algorithm on EMG data sets of the upper extremity of healthy people. Our twelve participants executed hand-reaching movements in multiple directions. Muscle synergies that were extracted from movements to the center of the reaching space could be generalized to synergies for other movement directions. This finding was also supported by the application of a weighted correlation matrix, the similarity index and the results of the K-means cluster analysis. This might reinforce the notion that the CNS flexibly combines a single set of small number of synergies in different amplitudes to modulate movement for different directions.**

***Index Terms*— Muscle synergy, non-negative matrix factorization (NMF), motor control, electromyography (EMG), hand-reaching.**

I. Introduction

THE large number motor skills applied by the motor system emphasize the complexity of controlling the musculoskeletal system [1]. A possible mechanism for achieving efficient and accurate control, despite the difficulties of controlling so many degrees of freedom, may rely on generating movement as combinations of a small number of invariant muscle patterns, commonly referred to as muscle synergies.

According to this notion, the nervous system controls task execution, by combining a discrete number of synergies, embedded within the brainstem and spinal cord [2], [3]. Each synergy, composed of fixed patterns of muscle activity, are scaled by time coefficients. Therefore, in each motor task the cortical neurons recruit synergies in different proportions, allowing muscles to be activated by more than one synergy [4].

The concept of synergies control emerged upon the observation that different leg postures of frogs resulted with constant force-field as a result of electrical stimulus to the spinal cord. In the same study the authors observed that when stimulating two different locations in the spinal cord, the resultant force field was the vector summation of each of the stimuli separately [3], [5]. Similar findings were also observed by different experimental methods such as cutaneous stimulation [2], [3] and NMDA iontophoresis [6]. The properties of synergies control and their localization in the spinal-cord and brainstem, was established in animal studies by applying different algorithms. The studies were performed in frogs [2], [7]–[12], cats [13], [14], [14], [15], and monkeys [16], [17].

An opposing principal for motor control by the central nervous system is single muscle control. A single muscle mechanism, may offer greater flexibility to facilitate a large repertoire of movement. Kutch *et al.* [18] investigated the endpoint forces exerted during isometric contraction for multiple directions at the index finger metacarpophalangeal joint. A force covariance's map was used to study the coordination strategy underlying force generation: flexible control of single muscles or fixed control by muscle synergies. The authors found support for the existence of flexible activation of single muscles rather than synergies control.

From a computational perspective, on the other hand, such a control mechanism might impose a substantial computational burden on the central nervous system. Additionally, this control model does not elucidate how the central nervous system copes with the redundancy of degrees of freedom. In other words, how the central nervous system selects the appropriate muscle composition for a vast movement repertoire. This argument may also be enforced by the observation that movement kinematics share common properties between individuals.

Rigorous studies establishing the existence of synergy control, have found that similar synergies may, to a large extent, reconstruct EMG muscle patterns that were recorded during natural behaviors, and EMG muscle patterns evoked by intracortical electrical stimulation [17]. Also Tresch *et al.* [19] contradicted the argument asserting that synergies are the default of the algorithm when they reported the existence of similar synergies extracted by different algorithms on the

Manuscript received November 16, 2016; revised June 21, 2017 and September 1, 2017; accepted October 30, 2017. Date of publication November 2, 2017; date of current version November 29, 2017. *(Corresponding author: Sharon Israely.)*

S. Israely and E. Carmeli are with the Department of Physical Therapy, University of Haifa, Haifa 3498838, Israel (e-mail: sharonis@mh.org.il; ecarmeli@univ.haifa.ac.il).

G. Leisman is with the National Institute for Brain and Rehabilitation Sciences, Nazareth 16470, Israel, and also with the School of Health Sciences, University of Haifa, Haifa 3498838, Israel (e-mail: g.leisman@alumni.manchester.ac.uk).

C. Machluf and T. Shnitzer are with the Faculty of Electrical Engineering, Technion–Israel Institute of Technology, Haifa 3200003, Israel (e-mail: chay.machluf@gmail.com; talush.s@gmail.com).

Digital Object Identifier 10.1109/TNSRE.2017.2769659

same dataset. In the context of localization of synergies, innovative studies using optogenetics confirmed the existence of molecularly defined motor synergy encoder (MSE) neurons in the mouse spinal cord, suggested that they function as a central node in neural movement pathways. Photo stimuli directed upon the MSE drove a fixed pattern of muscle activity, which was modulated according to a rosto-caudal location [20].

In order to investigate the properties of such a control mechanism in humans, it was necessary for researchers to prove robustness of synergies in different circumstances. Indeed, numerous studies have observed that a discrete number of synergies may account for a large fraction of the variances of the EMG data across different upper extremities tasks [21]–[23], force constraints [24], [25], movement [25], [26] or force direction [27], as well as in the lower extremities in walking and running [28], [29]. Others have reported similar results using isometric contractions for different directions in healthy [30] and in post-stroke individuals [31]. In everyday activity, however, hand-reaching movement is often executed in diagonal directions in three-dimensional space, and is not constrained to execution in a certain plain [25], [32] or by other task constraints [31].

In this study EMG signals from eight shoulder and arm muscles of healthy individuals were measured during hand-reaching movements in multiple directions in three-dimensional space. The robustness of a representative set of muscle synergies was investigated to explore the muscle synergies' capacity to modulate reaching movements for multiple directions. A modified version of the NMF algorithm was implemented by using a cross validation technique between each original data matrix for certain movement directions and the synergy matrices of all the other movement directions. We assumed that if there exists a certain set of synergies for controlling all the movements in space, then any combination between the original EMG data and any of the synergy matrices of other directions should be accurately reconstructed by our NMF algorithm.

II. Methods

A. Participants

Twelve healthy volunteers (mean age 68.6 ± 7.5 years) participated in the study. Seven participants were male and 5 female, 9 were right hand and three left-hand dominant. The study was approved by the University of Haifa Institution Review Board, and performed in accordance with the Declaration of Helsinki. All participants signed an informed consent form.

B. Equipment

The hand-reaching spatial device (Fig. 1) is an adjustable, simple tool allowing standardization of hand pointing movement for 9 different directions between different participants. It is composed of two vertical rods to which are attached three semi-circular shelves. Each shelf contains three movable pointing pins that can be adjusted left and rightward to accommodate the variable arm length of each participant.

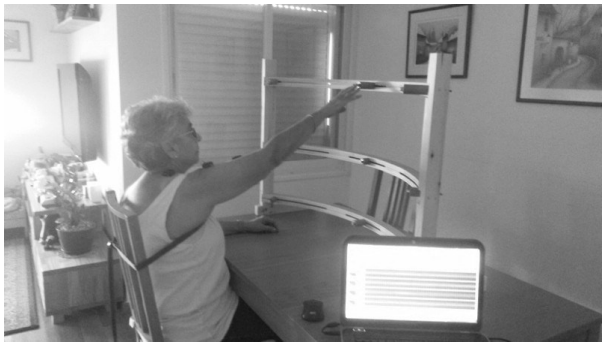

Fig. 1. The hand-reaching spatial device. Participants were asked to reach with their dominant hand to 9 different targets that were located in their maximum hand-reaching range of motion.

The lowest shelf was located 10 cm above the table, the middle was located 35 cm above the table and highest 55 cm above the table.

For each participant the hand-reaching device was located at the maximum hand reach distance in front of the tested shoulder. The side pins were located at a 45-degree angle to the shoulder joint to both sides. The arrangement of the targets on the hand-reaching device was designed to cover the majority of hand-reaching movements.

C. Electromyography

Surface EMGs were recorded (Trigno 8, Delsys, Boston, MA) from 8 muscles of the shoulder girdle and arm: trapezius, deltoid anterior, medial, and posterior fibers and pectoralis major; infraspinatus, biceps and triceps. Electrodes were placed in accordance with the guidelines of the Surface Electromyography for the Non-Invasive Assessment of Muscles–European Community Project (SENIAM) [33]. Maximum voluntary contractions (MVCs) were performed prior to data collection to verify correct electrode placement and for normalization. One-minute rest periods followed each MVC to limit the possibility of fatigue. EMG signals were band-pass filtered (20–450 Hz) and sampled at 2000 Hz.

D. Protocol

The MVC was measured by standard muscle testing [34]. Each subject sat in front of a table with his forearm resting in a comfortable position. The hand reaching device was located as indicated above. Participants were required to point to each target 5 times according to voice prompting that was activated every 10 seconds by the EMG software, for 45 pointing movements. The order of pointing targets was constant for all the participants. Fig. 2 illustrates the order of the targets for a person with right hand dominance. The order for a left hand dominant person was horizontally mirrored, but fixed in the vertical dimension such that target 1 was on the left down and target 9 was on the right-up.

E. Data Analysis

1) EMG Preprocessing: Data analysis was performed using Matlab (The MathWorks, Inc.). The EMG recording, for each

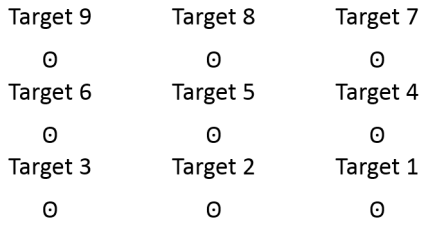

Fig. 2. Representation of the order and direction of the targets for a person with dominant right hand. The hand reaching device was located in a way that the 5th target was located in front of the shoulder. Targets 1, 4 and 7 were located to allow hand-reaching to 45° degrees of horizontal abduction. Targets 3, 6 and 9 were located to allow hand-reaching to 45° degrees of horizontal adduction.

participant and for each target, was organized as an 8-by-T matrix: $X^{8\times T}$ where 8 is the number of muscles and T is the number of samples in each target (for all repetitions). Let m be a row index in $X^{8\times T}$, indicating a specific muscle. The EMG's net noise was damped at 50Hz, followed by mean subtraction to remove offset errors:

$$X_m[n] \leftarrow X_m[n] - \frac{1}{T}\sum_{i=1}^{T} X_m[i], \quad m = 1\ldots 8 \tag{1}$$

This was followed by RMS calculation with overlapping windows of 50 samples (25 milliseconds around each time point).

$$X_m[n] \leftarrow \sqrt{\frac{1}{50}\sum_{i=(n-24)}^{(n+25)} (X_m[i])^2}, m = 1\ldots 8 \tag{2}$$

Each muscle was normalized, X_m, according to the nominal amplitude of the corresponding maximum voluntary contraction (MVC) test. Only the segments that contained muscle activity were extracted, using threshold-segmentation. This was performed by down-sampling along the time dimension by 1:10, followed by summing over the muscle dimension, resulting in a vector that represented the total activity of all muscles at each point in time:

$$X_{1\times T}[n] \leftarrow \sum_{m=1}^{8} \left(X_m^{downsampled}[n]\right)^2 \tag{3}$$

We then applied a moving average filter of length 100 samples in order to fill short gaps in muscle activity. A median filter of length 3000 (1.5 seconds) was applied to the smoothed muscle activity signal, in order to remove transient noise. The 1D signal, $X_{1\times T}[n]$, was segmented using a threshold, h, calculated according to: $h = \text{mean}(X_{1\times T}[n]) + 0.5 \times \text{variance}$. Only time-samples of $X_m[n], m = 1\ldots 8$ in which $X_{1\times T}[n] > h$ were taken, marked as the resulting matrices by V.

2) Degree of Muscle Activity for Different Movement Directions: The processed EMG of each muscle and for each movement direction was normalized according to 80% of the MVC. Therefore, the degree of muscle activation measure took values from zero to one. The mean of this processed EMG amplitude of activation (X_i^m) of muscle $m \in [1], [8]$ to target $i \in [1], [9]$ averaged for the whole group is illustrated in Fig. 3.

3) Identification of Muscle Synergies: The NMF algorithm originally used by Lee and Seung [35] was applied to identify muscle synergies and their activation weights. An EMG pattern recorded in hand-reaching movements was modeled as a linear combination of a set of N muscle synergies, each of which specified the relative level of activation across 8 muscles, and was activated by a time-varying activation coefficient [19], [30]:

$$V^{M\times T} \approx W^{M\times N} \cdot H^{N\times T} \tag{4}$$

Where V is the EMG data set matrix with M as the number of muscles (8 muscles), T as the number of time samples, W is the synergy matrix and H is the coefficient matrix. W is m × n is a matrix with n synergies, m is the number of muscles, and H is the n × t matrix of synergy activation coefficients. Thus, each column of W represents the weights of each muscle for a single synergy, and each row of H represents how much the corresponding synergy was activated or used to generate force. In this model, it is possible for each muscle to belong to more than one synergy and thus the EMG of any single muscle might be attributed to simultaneous or sequential activations of several muscle synergies.

The synergies and their activation coefficients were extracted by implementing the NMF iterative update rules in Matlab. Under these update rules, at each iteration, new estimates of W and H were calculated by multiplying the current estimates by factors depending on V and current estimates of W and H. This iterative estimation procedure was stopped after convergence of the reconstruction error according to the equation:

$$\varepsilon_w(t) = \sqrt{\frac{1}{N\times R}\left(\sum_{i,a}^{N,R} (W_t[i,a] - W_{t-1}[i,a])^2\right)} \tag{5}$$

where N × R is the number of elements in W (e.g – for 8 muscles and 4 synergies, N × R = 32), t is the iteration number, i is the number of muscles of W and a is the number of synergies in W. The algorithm was iterated until either: $\varepsilon_w(t) < 10^{-6}$ or $t = 500$,, whichever comes first.

4) Estimating the Optimal Number of Muscle Synergies: Two criteria were applied to determine the optimal number of synergies: (1) mean squared errors (MSE); [8]); and (2) the Variance Accounted For (VAF) [8], [36]. The optimal number of synergies was identified by the number of muscle synergies at which the VAF curve changed sharply according to the MSE value [8], [31]. We additionally considered that the optimal number of synergies should reliably represent a significant reduction of dimensionality of the muscle activation pattern. The first method suggested fitting portions of the VAF curve to straight lines using the least squares technique. Initially all data points on the VAF curve were included, and then the 2nd to 7th points, and so on until only the 5th and 7th points were included. The correct number of synergies could then be estimated as the first point on the VAF curve at which the linear fit of all points from that point to the 7th point produced a small MSE. Using the second method, the optimal number of synergies was defined as the minimum number of synergies

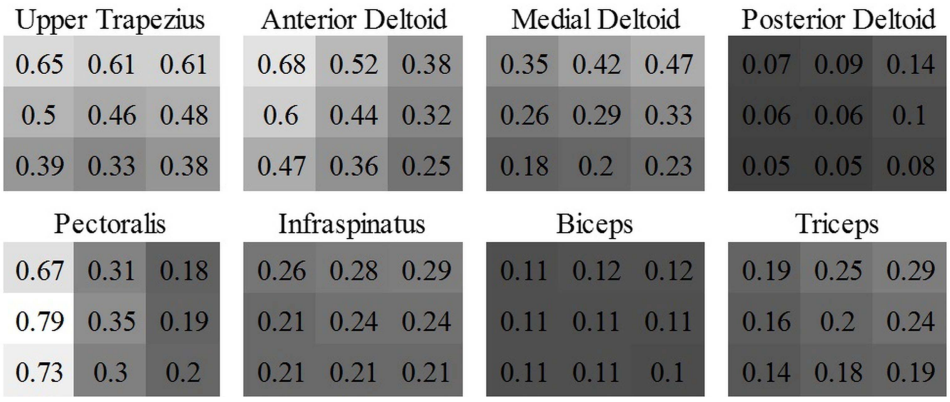

Fig. 3. Muscles activation levels across target direction. Bright colors indicate for higher level of activation, dark colors indicate for lower level of activation.

that achieved a mean VAF > 85%, with less than a 5% increase in the mean VAF upon addition of another synergy [36].

The NMF algorithm required the number of synergies extracted to be specified before the application of the algorithm. Therefore, for each data set, the VAF was calculated while changing the number of synergies from 1 to 7. The VAF was calculated using the equation according to d'Avella *et al.* [25] as follow:

$$VAF\,(H) = 100\% \times \left(1 - \frac{||V - WH||_2^2}{||V - \bar{V}||_2^2}\right) \tag{6}$$

Where V is the original matrix, and W and H are the derived, factorized matrices.

5) Building a Representative Set of Muscle Synergies: Our aim in this stage of analysis was to determine whether a set of synergies exist that control the tested reaching movement in space. Therefore, we investigated how movement in certain directions could account for movements in other directions. We pooled the EMG data for each movement direction separately across the 8 muscles and concatenated it for the whole sample. In that way the derived set of synergies would have had to account for the variance between different subjects, but would also have had to be specific for that direction alone. We applied the NMF separately for each movement direction according to the equation:

$$V_i \approx W_i \cdot H_i \tag{7}$$

where i is the target number, which corresponded to specific movement direction in space. In this stage of analysis V_i (the EMG matrix) was given as an input for each target, i ∈[1], [9], and matrices W_i and H_i were updated iteratively. The study procedure included reaching for 9 different target directions in space, allowing us to further investigate if there was a single set of synergies that could account for movements in other directions.

This was accomplished by using a cross-validation technique between the V_i matrices and the W_j matrices by applying a modified version of the NMF algorithm, followed by corresponding VAF calculation changing the number of synergies from only 3 to 5, and not from 1 to 7 based on the results of the NMF for all the participants and for all targets, as detailed in the results section. In the modified version of the algorithm, both V_i and W_j (the synergies matrix) were given as an input. Only the $H_{i,j}$ coefficients matrix of target i, was updated and outputted.

The cross-validation process of the modified NMF was carried out for each combination of a data matrix V_i (of target i) and a synergy matrix W_j (of target j), resulting in 9×9 matrices H_{ji} including V_i and W_i. For every i, j ∈[1], [9], we factorized V_i such that $W_j H_{ji} \approx V_i$.

The representative set of muscle synergies was chosen by calculating the VAF for each of the 9×9 factorizations:

$$VAF\left(H_{ij}\right) = 100\% \times \left(1 - \frac{\left||V_i - W_j H_{ij}\right||_2^2}{\left||V_i - \overline{V}_i\right||_2^2}\right) \tag{8}$$

assuming that consistent high values of $VAF(H_{ij})$ for a specific V_i may indicate that the synergies obtained from movements in this direction may accurately explain movement in other directions. Thus, for each predefined number of synergies, we received a 9×9 matrix (Fig. 6) in which each cell represented the accountability of a given synergy (row) to a specified direction (column). Each row in the resulting matrix represented the overall "performance" of the appropriate set of synergies, and so the row with the highest average VAF was chosen to be the representative set of synergies for the next stages of analysis.

6) Methods for Validating the Representative Set of Muscle Synergies: In order to validate the decision of choosing the representative set of synergies, three additional statistical methods were applied: 1) the Similarity Index; 2) Weighted Correlation Matrix and 3) K-means Cluster Analysis. The similarity index (SI in equation 9) was calculated using the Euclidian distance between the representative set of synergies (W^{rep}) and each of the W matrices of each participant and for each movement direction and then divided by six to be normalized to one as follows:

$$SI(rep, W) = \frac{\sum_{i=1}^{8}\sum_{j=1}^{3}\left|W_{i,j}^{rep} - W_{i,j}^{T}\right|}{6} \tag{9}$$

Where i ∈ [1], [8] was the muscle number, j ∈ [1], [3] was the number of synergies and T ∈ [1], [9] was the target direction number. Each W_i matrix was i × j matrix. Since the sum of

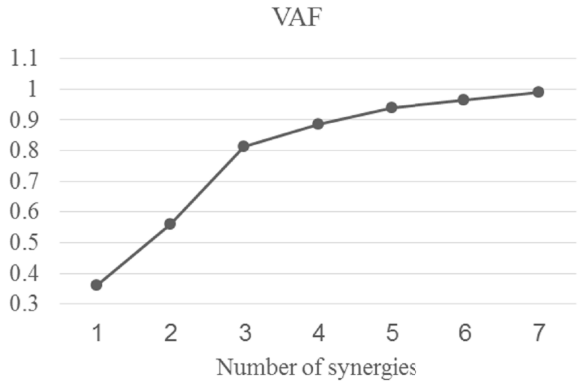

Fig. 4. VAF results as a function of the number of synergies. The NMF was applied after all the targets of each participant were concatenated and pooled for the whole sample.

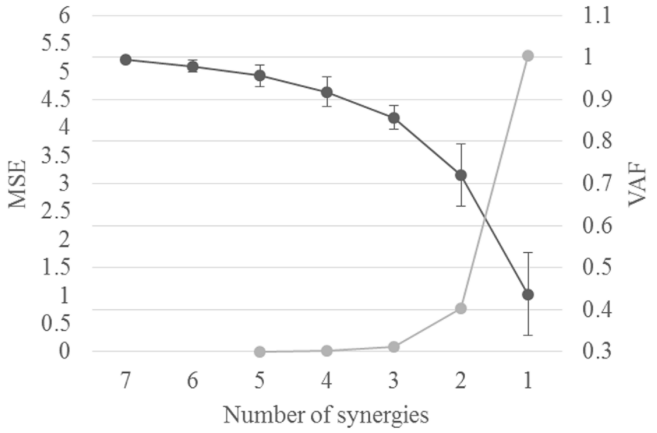

Fig. 5. Mean VAF and mean squared errors (MSE). For each participant the EMG data for all the target-directions were concatenated. The NMF was applied, changing the number of synergies from one to seven. The MSE was analyzed to assess the degree of linearity of the FAV curve. The MSE was calculated first including all data points on the curve in the fit, and then the 2nd to 7th points, and so on until only the 5th and 7th points were included. As the range of the fit moves toward the left side of the curve, the mean squared error (MSE) of the fit was expected to decrease because the VAF curve approaches a straight line as the number of synergies extracted increases. The correct number of synergies could then be estimated as the first point on the VAF curve at which the linear fit of all points from that point to the 7th point produces a small MSE.

each column in matrix W is one, so the maximal score for similarity between each two matrices was one. The similarity matrix is plotted in Fig. 7. The Weighted Correlation matrix (Fig. 6B) was calculated using the same W matrices of the participants, as described for the similarity index. For each participant, each of the nine W matrices was correlated to the other eight W matrices. The 12 correlation matrices of the whole group were averaged. Only statistically significant correlations ($p<0.05$) were calculated for the resultant weighted correlation matrix.

7) Discrimination Between Different Movement Directions Based on the Properties of Synergies: The K-means algorithm was applied to study whether the full activation coefficient properties of synergies may discriminate between different movement directions. The data used for the K-means were the H coefficient matrices of the cross validation procedure. Each V matrix of the whole group for each direction separately was decomposed by a standard NMF. Then the cross-validation procedure was carried out between each original V matrix and the W matrices that were extracted from all other directions. Therefore, the properties of the resultant H matrices may discriminate the V matrices that were decomposed. This was applied by using a limited number of constant features from the full activation coefficient matrices (H).

The selected features included 7 data points equally scattered on the H coefficient matrix, time to first peak and its amplitude, time to second peak and its amplitude and the total area under the curve. Peaks were defined using the 'MinPeakWidth' function of 500 data points in MATLAB. If either the first or second peaks did not exist, the algorithm substituted the missing data by the mean amplitude and middle time point of the matrix.

The K-means algorithm was applied for three different K values: nine, six and four. For each K value the algorithm was iterated 5 times using random centroids. In each running of the algorithm the accuracy of clustering was calculated using purity scores, and averaged for the 5 iterations. The purity was defined as the total number of data points that were classified correctly divided by the total number of data points, and multiplied by 100. The correct classification of a cluster was determined according to the most frequent index value in a row of the K-means analysis matrix (Fig. 8A).

8) Direction Modulation of Muscle Synergies: The properties of the synergies for different movement directions were investigated from two different perspectives. Firstly, once the representative set of synergies (W_j) was chosen, the EMG data for the whole group was concatenated for each direction separately and decomposed by the representative set of synergies. Then, we employed the means of the resultant activation coefficients matrices ($H_{ij}, when\ i \in [1],[9]$) for every target and plotted them according to the target directions (Fig. 9B according to Fig. 2), for each synergy separately.

Analyzing this plot allowed us to study the changes in mean amplitude of activation of synergies for different movement directions. Secondly, the functional role of each of the extracted synergies was investigated by plotting the full activation coefficient matrices (H) (Fig. 10). Accordingly, these temporal activation properties would help to distinguish between different movement- directions.

III. Results

A. Directional Activation Muscles

Fig. 3 illustrates the activation level of each muscle compared to the activation level of the same muscle on the other targets, and relative to the other muscles at the same target. Therefore, the values indicate the dominance of each muscle compared to other muscles for the same movement direction, which also related to the other movement directions.

Three dominant muscles for pointing movements were the pectoralis, anterior deltoid and the trapezius. Each of these muscles, however, demonstrated different patterns of activation for different directions. The trapezius was activated as the movement direction became higher, regardless whether

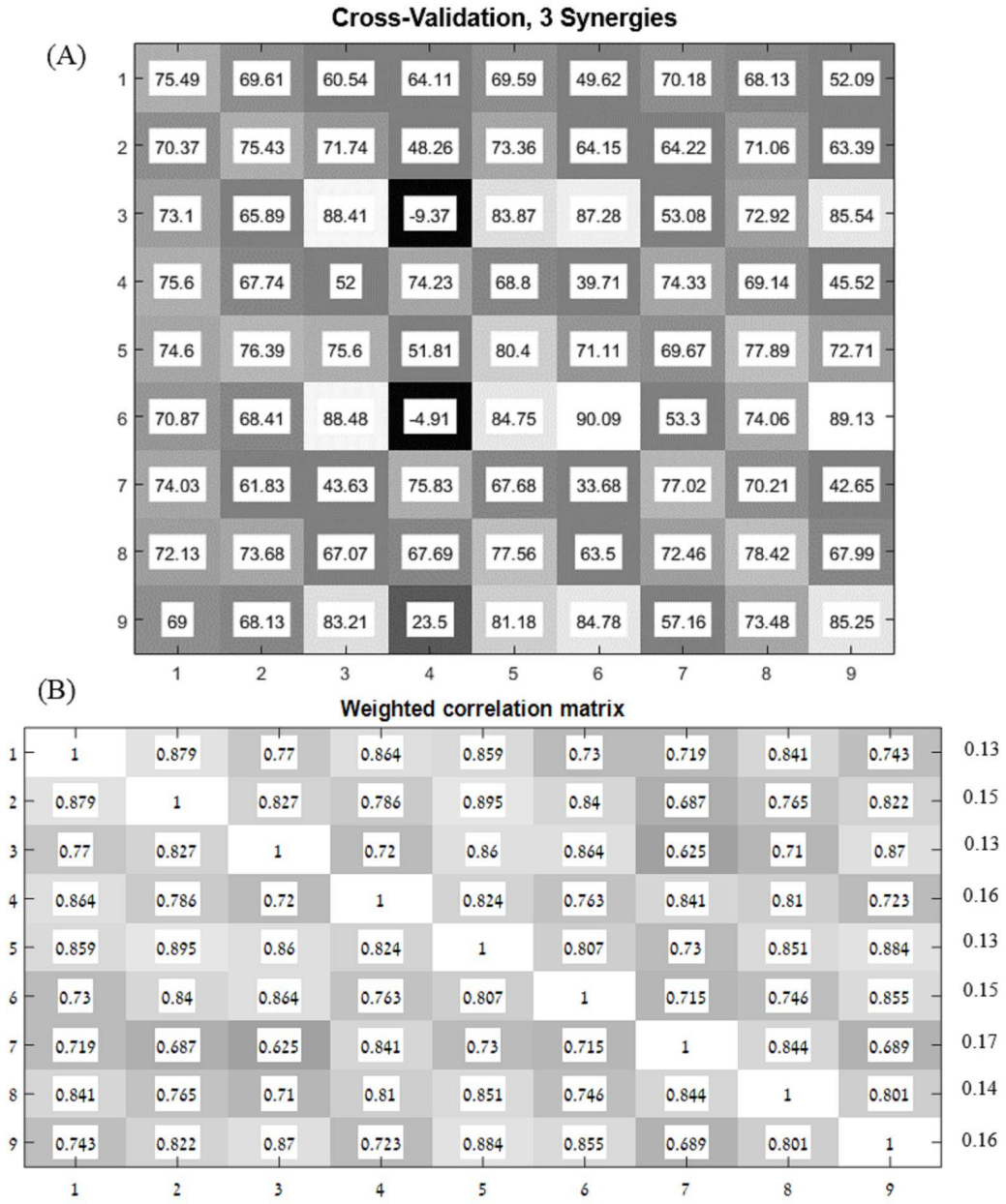

Fig. 6. Cross-validation matrix results for three synergies (A), and corresponding correlation matrix (B). The values in each cell in (A) represents the VAF values in percentages, of the corresponding modified NMF. For example: application of the modified NMF between V_5 and W_6 resulted with corresponding VAF of 84.75%. The VAF values are correspond to the cross-validation between each original V_i matrix and all the other W_j matrices, resulted with 9×9 matrix. The correlation matrix in (B) takes values from 1 to -1. The correlations were computed for each participant separately, between all the combinations of movement directions, and averaged for the whole group ($p<0.05$). The averaged standard deviations of the correlations were averaged for each row and presented on the right of the correlation matrix in (B).

it was directed to the side of the body or across the body. The pectoralis activation was higher as the movement was directed across the body. The anterior deltoid activation level demonstrated a combined pattern in which the activation values rose for higher movements and across the body. The medial deltoid, triceps and the infraspinatus had moderate to low levels of activation across all the targets. In these three muscles there was a trend toward higher activation levels for higher movements and to the side of the body. The biceps and the posterior deltoid, on the other hand, displayed very low level of activation across all of the target directions.

B. The Optimal Number of Synergies for Any Direction of Movement

The quality of the NMF to reconstruct the EMG data was evaluated by two measures: MSE and VAF. Fig. 5 illustrates the changes in the VAF and MSE values as a function of the number of synergies. Calculating the MSE from synergy 3 to 7 yielded an MSE value of 0.084 and from synergy 4 to 7 MSE of 0.014 and from 5 to 7 an MSE of 9.4^{-4}.

The observed MSE values were significantly higher than the values reported by others [8], [31], suggesting a decreased similarity of the VAF curve to a straight line. The VAF's were

calculated twice: First, the EMG data of each participant was concatenated for all the targets and then was pooled for the whole sample, before the application of the NMF (Fig. 4).

Second, the NMF and a corresponding VAF was applied separately for each participant, (Fig. 5). We additionally considered that the extracted synergies should represent a significant reduction of dimensionality of the muscle activation pattern. From this perspective, given that two muscles, the posterior deltoid and biceps were activated to a lower extent, three synergies were chosen to represent the optimal number of synergies. Fig. 5 illustrates the two criteria, which were applied to determine the optimal number of synergies, the mean VAF and the MSE. Three synergies accounted for 0.856 ±0.286 of the data variances, with respective MSE of 0.084. Four synergies accounted for 0.917±0.034 of the data variances, with respective MSE of 0.014. Therefore, the optimal number of synergies was defined as the minimum number of synergies that achieved a mean VAF > 85%, with less than a 5% increase in mean VAF upon addition of another synergy [36].

C. Building a Representative Set of Muscle Synergies

Setting the optimal number of synergies doptimal to 3, we used the cross-validation matrix to study which movement direction might best represent other movement directions, assuming that this set of synergies might be optimally modulated to reconstruct the muscle activity from other movement directions. Fig. 6 illustrates the VAF values of the cross-validation matrix V_i of each target direction using the W_j matrix of the other 8 target directions. The values on the diagonal of the matrix represent the results of the standard NMF of V_i with W_i. According to our assumption, the higher the VAF values in Fig. 6, the higher the chance that a specific movement direction could be generalized to explain movements in other directions. In order to validate this assumption and justify the selection of the representative set of synergies, we additionally calculated a Weighted Correlation matrix (Fig. 6B), the Similarity Index matrix (Fig. 7) and also employed the K-means algorithm.

The cross-validation between W_5 and all other V matrices, i.e. row number 5, yield the highest mean VAF values of 72.241%, which was consistent with the highest mean correlation value of 0.838 in row 5 Fig. 6B. These two findings may justify the selection of W_5, which was directed to the middle of the reaching space (Fig. 2) as the representative set of synergies. These findings were equivocally justified according to the non-significant results of the similarity index calculation (Fig. 7).

The VAF values of two cells were negative, both resulted from data matrix V_4 and synergy matrices W_3 and W_6. The modified NMF between V_4 and W_9 also resulted with VAF of 23.5% percent. A possible explanation why V_4 was not compatible with W_3, W_6 and W_9 refers to the relative complexity inherent in movement across the body, such that were carried out to targets 3, 6 and 9. This issue is further discussed in the discussion section. Based on the above finding we also assume that a reaching movement to the center of the reaching space, (i.e. target 5) can be best generalized to reaching movements in other directions.

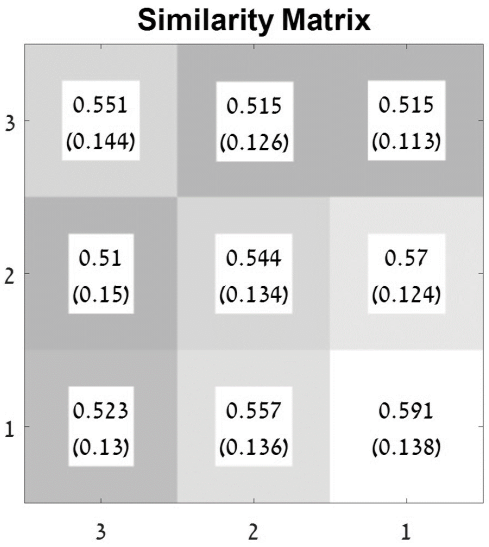

Fig. 7. The similarity matrix (Mean, standard deviation). The distance between the representative synergy matrix W and the synergy matrices of each of the participants for all movement directions were calculated and averaged for each movement direction. The similarity value in each cell takes values from zero for total identity between the calculated matrices, or one to totally different matrices.

Fig. 7 illustrates non-significant differences between the similarity of each set of synergies for a particular direction and the representative synergy. The similarity between the representative set of synergies and synergies for other movement directions were consistently moderate across the target directions. Since the correlation matrix resulted with high correlation values, it was expected that also the similarity index would result in high similarity scores between different movement directions.

The equivocal results of the similarity matrix, emphasize the differences between the correlation measure and the similarity index measure, which are discussed in the discussion section.

D. Discrimination Between Different Movement Directions Based on Synergies Properties

The main concern of using an unsupervised learning approach to cluster the data, based on the activation of synergies, was whether the different movement directions can be discriminated based on the activations of 3 synergies. If it does, it may reinforce the assumption that a small number of synergies are modulated to control movement for different directions.

The mean precision of clustering using 9 clusters was 80.246%, for 6 clusters was 87.407% and 88.888% for 4 clusters. Fig. 8 illustrates an example of 6 clusters from a single iteration of the K-means. The data used for the K-means were the coefficient matrices of the cross validation procedure. Therefore, the input data included 81 rows (samples). Accordingly the length of the index vector of the algorithm was 81 data points. The resultant index vector was re-ordered to correspond to the cross-validation matrix in Fig. 6. As Fig. 8 illustrates, different movement directions can be accurately discriminated by the K-means algorithm. This is especially

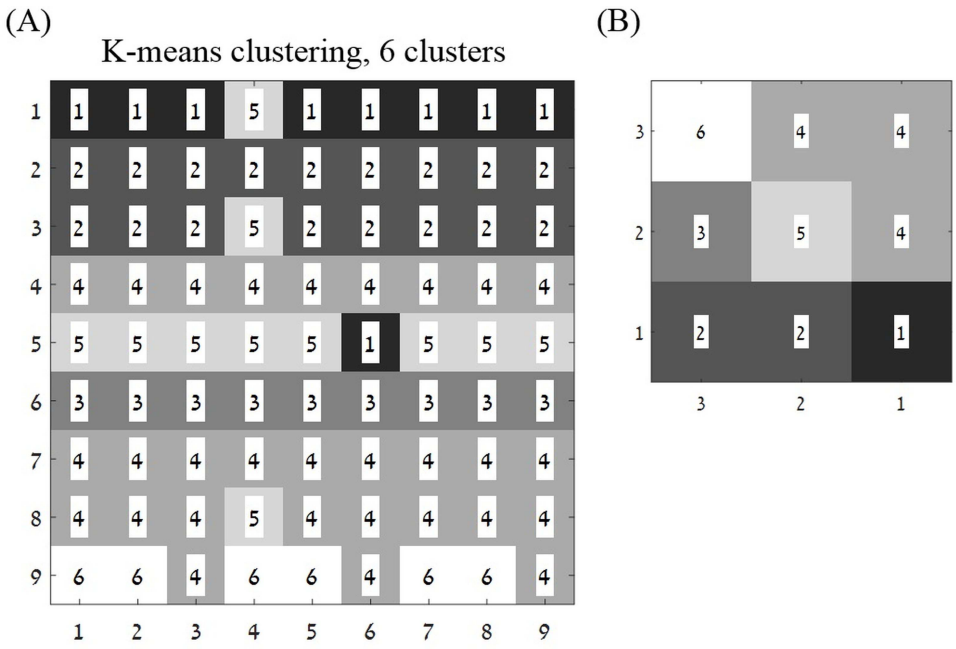

Fig. 8. Demonstration of discriminating synergies according to six clusters, applied by the K-means algorithm. The K-means algorithm was applied to study whether the full activation coefficient properties of synergies may discriminate between different movement directions, using the *H* coefficient matrices of the cross validation procedure. The properties of the resultant *V* matrices may discriminate the *V* matrices that were decomposed. The K-means algorithm was applied by using a limited number of constant features from the full activation coefficient matrices (*H*). In each running of the algorithm the accuracy of clustering was calculated using purity scores, and averaged for the 5 iterations. The purity was defined as the total number of data points that were classified correctly divided by the total number of data points, and multiplied by 100. The correct classification of a cluster was determined according to the most frequent index value in a row of the K-means analysis matrix. The values in each cell in (A) and (B) represent the index given by the algorithm. The accuracy of clustering in (A) was calculated to be 91.358% in this example, using the purity scores, according to the reference clusters in (B). For example, the 4th row in (A) refers to the 4th target (see this figure in (B) and also Fig. 2), demonstrates 100% purity. In other words, even when using an unsupervised approach, the algorithm discriminated all the *H* matrices that were extracted from the EMG data toward target 4. Row 9, on the other hand, demonstrates only 66% purity. Matrix (B) illustrates the clusters indexes according to the spatial arrangement of targets according to Fig. 2.

applied to targets that are located in the corner edges of the reaching space.

E. Direction Modulation of Muscle Synergies

The reconstruction of the muscle patterns by synergy combination for movements in different directions occurs by recruiting the synergies in different amplitudes for each movement direction (Fig. 9B). Each synergy and its level of activation was displayed separately across the 9 targets. The values in each cell in Fig. 9B are the mean activation coefficients of the *H* matrices, representing the intensity in which each synergy is activated for every direction. The synergy matrix (*W*) in Fig. 9A illustrates the intensity of activation of muscles in each synergy.

Synergies 1 and 3 increasingly activated as the direction of movement becomes higher. Synergy 2 was increasingly activated for movements involving horizontal adduction, i.e. movement across the body. None of the three synergies preferred direction of activation incorporated a downward vector component. Similarly to Fig. 3, the synergy matrix indicates that the biceps and the posterior deltoid muscles were not significantly activated during the reaching tasks. The anterior deltoid was dominantly activated in synergies 1 and 2, which demonstrate its role as a prime mover in hand-reaching. The preferred directions of activation of synergies 1 and 3 were similar, although the muscles composing each of the synergies was significantly different.

Fig. 9B also illustrates the degree of activation of synergies for each movement direction. The level of activation of synergies increased with shoulder flexion and horizontal adduction, and decreased in movements with mild shoulder flexion and horizontal abduction. For example, shoulder flexion with adduction (Target 9) was generated by recruiting all the three synergies in high intensity, although the second synergy was activated to a similar amplitude for targets 6 and 3. Movements involving mild shoulder flexion with abduction (Target 1), on the other hand, were generated by recruiting all the three synergies in low intensities.

In terms of temporal characteristics, Fig. 10 demonstrates the time properties of synergies activation coefficients for different movement directions of participant number 11. Synergy 1 sustained a similar time pattern across movement directions peaking around 2000msec. In terms of amplitude of activation, synergy 1 was significantly more activated over the other two synergies, especially for targets 7, 8 and 9. This also was related to which of the muscles composed this synergy. In this case it was comprised of the two heads of the deltoid and the triceps muscles. Additionally, the peak of activation of this synergy in the middle of the task execution also matches with the increased torques applied on these muscles while the limb is fully extended.

Synergy 2 exhibited high activation values for movement across the body (targets 3, 6 and 9), but negligible activation for targets 1, 4 and 7. In terms of timing of activation,

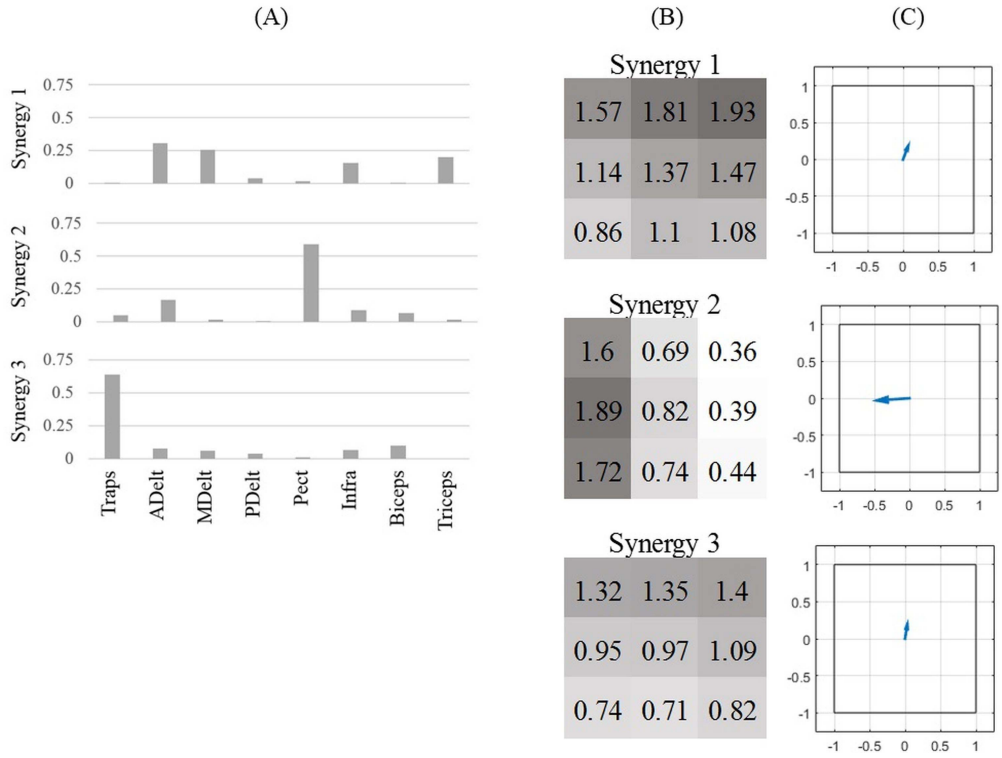

Fig. 9. Synergies activations and preferred direction. (A) The representative synergies matrix (W). Dark colors indicate for higher level of activation, Bright colors indicate for lower level of activation. The mean activation coefficient matrices *H* (B), and the preferred direction of activation of the corresponding synergies (C). The values in synergy matrices A are summed to a value of one. The values in matrices B represent the mean activation coefficients of the NMF, therefore these values might be above one.

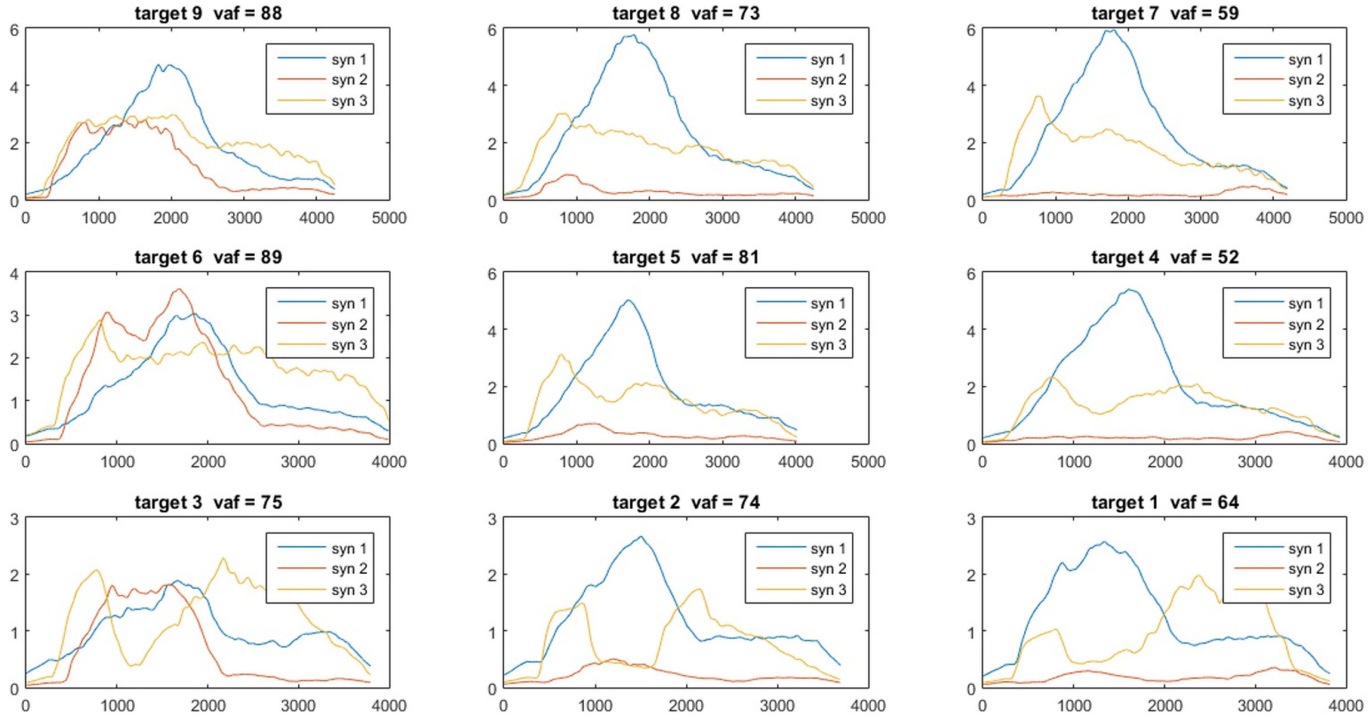

Fig. 10. The full activation coefficient matrices (*H*) to each movement direction, of participant 11. The spatial order of targets were according to Fig. 2. The three synergies demonstrated different time- patterns of activation for each of the targets. Each of the synergies differently modulated for different targets. In each subplot the x-axis refer to time and the y-axis to the activation coefficient value. Therefore, the values of the y-axis were not normalized.

synergy 2 was mainly activated in the first 2000 msec. from onset, which refers to the reach out phase and not returning the hand back close to the body. The third synergy demonstrated a type of bi-phasic activation pattern, assumingly due to higher activation of the trapezius muscle at the beginning of the reaching to distant the hand from the body, and

again at the beginning of bringing the hand back toward the body.

IV. Discussion

In this study, the muscle patterns of hand-reaching in three dimensions for multiple directions were decomposed into small numbers of muscle synergies by applying the NMF algorithm. We particularly aimed to investigate how muscle synergies that were extracted from a certain movement direction could be generalized to movements in other directions, and particularly whether a single set of synergies might be modulated to reconstruct movements in other directions.

Therefore, a modified version of the NMF was applied using a cross-validation procedure between each original dataset from each movement direction with the synergy matrices from movements to all other directions. We additionally applied three different analyses to support the existence of representative sets of synergies in non-stroke individuals. It was hypothesized that high VAF values and high correlation values, and an ability to discriminate between different directions may successfully demonstrates the spatial generalizability of a single set of synergies to multiple movement directions.

According to our initial criteria for determining the optimal number of synergies, three synergies accurately reconstructed the EMG data, both for the whole sample and for a single participant without discriminating between different movement directions. Additionally, a major concern when determining the optimal number of synergies is to gain a significant dimensionality reduction. Since two muscles were activated to lower extent, so choosing four synergies was not appropriate from this perspective, even if the other measures (VAF and MSE) would support it. In order to address this issue in future studies, it is recommended to measure the EMG activity of more than 8 muscles, especially when studying movement tasks that might involve the same group of muscles. Adhering to the study objective, a modified NMF was applied using a cross-validation technique. The results of the cross-validation procedure were not consistent among the different target locations. Our results demonstrated moderate to good VAF values using synergies that were extracted from hand-reaching movements toward the mid-sagittal plane (targets 2, 5 and 8) and from movements involving horizontal abduction (targets 1,4 and 7). Movement directions across the midline (targets 3, 6 and 9) yielded poor VAF values. The negative and decreased values presented in the cross-validation matrix between rows 3, 6 and 9 and column 4 resulted from the mathematical definition of the VAF value. Since the denominator of the VAF value contained the actual data point subtracted by the mean of the data points, this may have resulted in small denominator values. Accordingly, the whole value that was subtracted from one might be close to or larger than one. Therefore, the VAF index may have also produced negative values. In the next paragraph we discuss and explain our findings.

Possible explanation for the incompatibility between V_4 with W_3, W_6 and W_9 refers to the relative complexity inherent in movement across the body. Moving the hand across the midline may conceal several implications that are not likely to exist in movements to the ipsilateral side. From a functional point of view, executing unilateral reaching movements across the midline using the contralateral hand is less efficient than with the ipsilateral hand [37], and requires coordinated function to process the visual information while simultaneously moving the limb [38], [39]. Two contradicting ideas may explain the difficulties of moving the hand across the midline. First, it was suggested that even in adulthood, humans prefer to reach with their ipsilateral hand [40]. On the other hand, it was reported that locating objects across the mid-space encourages the use of the dominant arm. This suggests that reaching across the midline represents increasing levels of task difficulty [41].

From neuroanatomical framework the majority of the corticospinal tract (CST) fibers cross the midline, so movement of the right hand is mediated by the left hemisphere. The sensory information to the eye, on the other hand, is transformed by both unilateral and cross fibers as vision is processed bilaterally, (i.e. the left eye receives visual information that arises from both sides of visual space). When an object is located at the right side of the body, the task would apparently be executed by the right hand. This task execution of the right hand would be processed by the left motor cortex and be mediated thought the activation of the CST.

At the same time the left cortex will processes the visual information that is originated from the right visual field. Now, suppose the right hand need to be cross the midline to the contralateral side (the left side of the space). The efferent messages will still be processed by the left hemisphere through the CST. The processing of the visual information, on the other hand, will now switch sides to be processed by the right hemisphere. In fact, the same hemisphere for motor outputs mediates an ipsilateral motor task as it is for visual processing. Contrarily, different hemispheres for motor outputs and visual processing respectively would process movement across the midline. We assume that this might be a crucial factor affecting the motor performance for movements that were executed across the midline. This, in turn might affect the ability to generalize from a movement across the midline to other movement directions.

Two studies reported that hand-reaching for different directions might be successfully represented by scaling a small number of muscle synergies [26], [42]. Among these two studies Muceli *et al.* [42] used cross-validation techniques to investigate how synergies from a certain movement direction may describe movements to other directions. The authors reported that a single set of synergies that were extracted from a single movement direction could poorly reconstruct EMG data collected from reaching movement to other directions.

Extracting synergies from a combination of three targets, however, allowed good reconstruction of the EMG recorded from movements that were executed to other directions. Consistent with our findings, visual inspection of the results (Figure 6 in [42]) might imply that the reconstruction errors were more pronounced for targets that were located across the midline (8, 9, 10 and 11) and less for ipsilateral targets (2, 3 and 5).

Apparently, also the different study settings might explain differences in the results of the above study and in ours.

In Muceli *et al.* [42] the reaching tasks were performed in two dimensions, and were executed within a limited range of motion of 15 cm. Moreover, none of the targets were located in the mid-space, limiting the ability to describe movements scattered in space by movement to the center of the reaching space. Possibly more demanding tasks in the three dimensional space would highlight the differences between ipsilateral reaching and reaching across the body. In another study, Semprini *et al.* [27] applied the space-by-time NMF algorithm to decompose wrist movements in three dimensions, under four different force conditions. The authors reported increasing activation coefficient values corresponding to higher forces applied by the robotic device, which is consistent with our findings in which reaching movements that were directed to higher targets, especially those involving horizontal adduction, scaled by higher activation coefficients. Additionally, the similarity between the synergies of each of the participants was correlated with the average set of synergies, validated as a representative set of synergies. The authors suggested that high-moderate correlation coefficient values allow the average set of synergies to be set as a representative set of synergies.

In this study, the interpretation of the low VAF values in the cross-validation between the synergy matrices W of targets 3, 6 and 9 and the data matrix V_4 refer only to the ability or inability to generalize synergies from one movement direction to other directions. Validating our decision to use a representative set of synergies for decomposing EMG data from different movement directions, we applied three additional statistical methods. High correlation values illustrated in Fig. 6B and reliable synergy-based discrimination between different directions validating the existence of a representative set of synergies. The latter means that if given an EMG data matrix form an unknown movement direction, decomposition of this matrix by a representative set of synergies might make it possible to reveal the direction of that movement, based on features from the resultant full coefficient matrix.

In contrast to the correlation matrix, the similarity values between different directions were moderate. The inconsistency between these two measures may have a number of possible explanations. Firstly, the correlation index measures only the "global trends" between two data measures, and not the actual values of each of the measures. Accordingly, the correlation might be optimal even if the actual values of measures are far from each other. In this case, on the other hand, the similarity value would be closer to one (less similarity). Therefore, it is possible that the same two data matrices would result with high correlation values but low similarity. Secondly, the similarity index described the capacity to modulate the activation of synergies for different movement directions. It was expected, therefore, that non-stroke individuals would sustain this ability to modulate the activation of synergies, which in turn might be characterized by decreased similarity values. In keeping with this line of reasoning, one might argue that increased similarity between synergies might express stereotyped movement patterns, or impaired ability to modulate synergies, which often exists in post-CNS lesions. Further studies should explore whether the degree of motor impairment might be indicated by impaired ability to modulate synergies for different movement direction, according to laws of similarity values. In order to resolve the inconsistency between the similarity index and the correlation matrix, future studies with non-stroke individuals might also consider to measure the EMG activity from larger number of muscles.

Using an unsupervised leaning approach, we aimed to study whether different movement directions might be discriminated based on the modulation of representative sets of synergies. Previous studies also applied the K-means algorithm [43], or hierarchical cluster analysis to study the shared synergies between different individuals [22], [23], [25], [31]. Other classification algorithms such as Linear Discriminant Analysis (LDA), Artificial Neural Networks (NN), one-vs-all Support Vector Machine (SVM) were used to discriminate between different locomotion modes [44]–[46], LDA and Muscle Synergy Discrimination (MSD) for discriminating between hand movements [47]. Other studies that characterized synergies according to their directional tuning [24], [26] suggested that scaling of synergies might capture the differences between different movement directions [26] in hand-reaching tasks as well as in isometric force generation for multiple directions [31].

Further investigating the properties of the synergies, a representative set of muscle synergies was determined according to the highest mean VAF of W_i in the cross validation matrix. Therefore, W_5 which was represented by the 5^{th} row in Fig. 6 was chosen to study the properties of synergies that were extracted form hand-reaching movements for multiple directions. Specifically the analyses were focused on the muscle composition of the synergies, the directionality of activation of synergies and the activation timing of the synergies.

Fig. 9 illustrates the muscle composition of the synergies and the direction of activation of the synergies. In most cases, it demonstrates consistency between the functional role of the muscles composing the synergy and the property of the synergy itself. Intuitively, the preferred direction of activation of a synergy will be compatible with mechanical force directions of the muscles composing it. A muscle may act as a prime mover in a synergy when the target is well aligned with that muscle's mechanical action. For other target directions, the same muscle will act as part of a group of co-activated muscles [18]. Indeed, the study by Berger and d'Avella demonstrated that the fourth synergy was mainly composed of triceps muscle activation and the third synergy was primarily activated by the pectoralis major [24] (please refer to [24] Fig. 2). Compatible with the above studies, synergy 2 (Fig. 9) was dominantly activated by the pectoralis muscle. Accordingly, its preferred direction was directed across the body, similar to the pectoralis force direction. Although this line of reasoning is more compatible with flexible muscle control than synergy control [24] this concept was mainly demonstrated on a single joint force production [18], and not necessarily can be generalized to multiple joint movements. Therefore, in terms of which control strategy is mainly engaged during hand-reaching, additional studies should investigate these two opposing control mechanisms.

An interesting finding is illustrated in Fig. 9C in which two synergies share similar preferred direction despite a marked

difference in the muscles composing these synergies. In order to understand this finding, it was necessary to define the preferred direction of a synergy as the direction of movement in which a synergy would be recruited the most. This is in contrast to an alternative definition in which the preferred direction refers to the direction of movement that would be generated as a result of activating a synergy. In this context it is reasonable that two synergies with different muscle composition will share the same preferred direction. Previous studies have shown that different synergies may share similar preferred direction of activation ([14] Fig. 7B, and [30] Fig. 7A [14], [30]), in contrast to others who reported different preferred direction of activation of synergies [24]. Furthermore, since the directional modulation of synergies was analyzed only in the frontal plain, it is possible that differences within the sagittal plain between synergies 1 and 3 were concealed (Fig. 9C).

Another concern regarding the direction of activation of synergies is whether it is possible that none of the preferred synergy directions were directed downward as shown in Fig. 9C. A critical factor influencing the preferred direction of synergies is the muscle composition that is required to be recruited to accomplish the task. Since any reaching movement is constrained by gravity forces, the muscle composition for executing reaching will probably involve only upward force vectors. Even during the lowering phase of the hand, the muscles exert eccentric contraction to resist gravity. The preferred direction of activation expresses the relative forces that were exerted to accomplish reaching tasks that were distinguished by the height of the target. Since increased force production is necessary for reaching movement above shoulder height, it is reasonable to receive a preferred upward synergy direction vector. Previous studies demonstrated that preferred synergy directions were pointed downward due to application of downward isometric force production [24], [30]. We found no research that analyzed the preferred direction of activation of synergies that were extracted from normal hand-reaching movement. We assume that downward preferred direction of synergies would be reasonable in tasks involving downward force vectors.

V. Conclusions

This study establishes the nature of limb movement control by modulation of a small number of synergies for reaching movements in different directions. The main finding of this study was that a single set of synergies that were extracted from hand-reaching directed to the center of the reaching space could reasonably be generalized to reconstruct data for other movement directions. This is a significant finding supported by the results of the weighted correlation matrix (Fig. 6B), the similarity matrix (Fig. 7) and K-means clustering (Fig. 8). We assume that with larger numbers of participants, the application of the cross-validation procedure may lead to a more rigorous representative set of synergies that allow the generalizability for different movement directions. Knowing in advance the intended direction of movement, although not necessarily executed accordingly, in people who sustained a CNS lesion, may be used to facilitate voluntary movement through synergy-based biofeedback techniques from the unaffected extremity or from a representative set of muscle synergies.

Acknowledgment

The authors thank Nimrod Peleg, Prof. Ronen Talmon and Jonathan Brokman of the Faculty of Electrical Engineering, at the Technion Israel Institute of Technology, Haifa, Israel for their professional consultation regarding the development of the algorithm.

References

[1] E. Bizzi and R. Ajemian, "A hard scientific quest: Understanding voluntary movements," *Daedalus*, vol. 144, no. 1, pp. 83–95, 2015.
[2] C. B. Hart and S. F. Giszter, "Modular premotor drives and unit bursts as primitives for frog motor behaviors," *J. Neurosci.*, vol. 24, no. 22, pp. 5269–5282, Jun. 2004.
[3] M. C. Tresch, P. Saltiel, and E. Bizzi, "The construction of movement by the spinal cord," *Nature Neurosci.*, vol. 2, no. 2, pp. 162–167, 1999.
[4] T. Drew, J. Kalaska, and N. Krouchev, "Muscle synergies during locomotion in the cat: A model for motor cortex control," *J. Physiol. Lond.*, vol. 586, no. 5, pp. 1239–1245, 2008.
[5] E. Bizzi, F. A. Mussa-Ivaldi, and S. Giszter, "Computations underlying the execution of movement: A biological perspective," *Science*, vol. 253, no. 5017, pp. 287–291, Jul. 1991.
[6] P. Saltiel, K. Wyler-Duda, A. d'Avella, M. C. Tresch, and E. Bizzi, "Muscle synergies encoded within the spinal cord: Evidence from focal intraspinal NMDA iontophoresis in the frog," *J. Neurophysiol.*, vol. 85, no. 2, pp. 605–619, Feb. 2001.
[7] A. d'Avella, P. Saltiel, and E. Bizzi, "Combinations of muscle synergies in the construction of a natural motor behavior," *Nature Neurosci.*, vol. 6, no. 3, pp. 300–308, 2003.
[8] V. C. K. Cheung, A. d'Avella, M. C. Tresch, and E. Bizzi, "Central and sensory contributions to the activation and organization of muscle synergies during natural motor behaviors," *J. Neurosci.*, vol. 25, no. 27, pp. 6419–6434, Jul. 2005.
[9] V. C. K. Cheung, A. d'Avella, and E. Bizzi, "Adjustments of motor pattern for load compensation via modulated activations of muscle synergies during natural behaviors," *J. Neurophysiol.*, vol. 101, no. 3, pp. 1235–1257, Mar. 2009.
[10] A. d'Avella and E. Bizzi, "Shared and specific muscle synergies in natural motor behaviors," *Proc. Nat. Acad. Sci. USA*, vol. 102, no. 8, pp. 3076–3081, Feb. 2005.
[11] J. Roh, V. C. K. Cheung, and E. Bizzi, "Modules in the brain stem and spinal cord underlying motor behaviors," *J. Neurophysiol.*, vol. 106, no. 3, pp. 1363–1378, Sep. 2011.
[12] S. Giszter, V. Patil, and C. Hart, "Primitives, premotor drives, and pattern generation: A combined computational and neuroethological perspective," *Prog. Brain Res.*, vol. 165, pp. 323–346, Dec. 2007.
[13] L. H. Ting and J. M. Macpherson, "A limited set of muscle synergies for force control during a postural task," *J. Neurophysiol.*, vol. 93, no. 1, pp. 609–613, Jan. 2005.
[14] G. Torres-Oviedo, J. M. Macpherson, and L. H. Ting, "Muscle synergy organization is robust across a variety of postural perturbations," *J. Neurophysiol.*, vol. 96, no. 3, pp. 1530–1546, Sep. 2006.
[15] N. Krouchev, J. F. Kalaska, and T. Drew, "Sequential activation of muscle synergies during locomotion in the intact cat as revealed by cluster analysis and direct decomposition," *J. Neurophysiol.*, vol. 96, no. 4, pp. 1991–2010, Oct. 2006.
[16] S. A. Overduin, A. d'Avella, J. Roh, and E. Bizzi, "Modulation of muscle synergy recruitment in primate grasping," *J. Neurosci.*, vol. 28, no. 4, pp. 880–892, Jan. 2008.
[17] S. A. Overduin, A. d'Avella, J. M. Carmena, and E. Bizzi, "Microstimulation activates a handful of muscle synergies," *Neuron*, vol. 76, no. 6, pp. 1071–1077, 2012.
[18] J. J. Kutch, A. D. Kuo, A. M. Bloch, and W. Z. Rymer, "Endpoint force fluctuations reveal flexible rather than synergistic patterns of muscle cooperation," *J. Neurophysiol.*, vol. 100, no. 5, pp. 2455–2471, Nov. 2008.
[19] M. C. Tresch, V. C. K. Cheung, and A. d'Avella, "Matrix factorization algorithms for the identification of muscle synergies: Evaluation on simulated and experimental data sets," *J. Neurophysiol.*, vol. 95, no. 4, pp. 2199–2212, Apr. 2006.

[20] V. Caggiano, V. C. K. Cheung, and E. Bizzi, "An optogenetic demonstration of motor modularity in the mammalian spinal cord," *Sci. Rep.*, vol. 6, p. 35185, Oct. 2016.
[21] V. C. K. Cheung, L. Piron, M. Agostini, S. Silvoni, A. Turolla, and E. Bizzi, "Stability of muscle synergies for voluntary actions after cortical stroke in humans," *Proc. Nat. Acad. Sci. USA*, vol. 106, no. 46, pp. 19563–19568, Nov. 2009.
[22] V. C. K. Cheung *et al.*, "Muscle synergy patterns as physiological markers of motor cortical damage," *Proc. Nat. Acad. Sci. USA*, vol. 109, no. 36, pp. 14652–14656, Sep. 2012.
[23] E. García-Cossio, D. Broetz, N. Birbaumer, and A. Ramos-Murguialday, "Cortex integrity relevance in muscle synergies in severe chronic stroke," *Frontiers Hum. Neurosci.*, vol. 8, p. 744, Sep. 2014.
[24] D. J. Berger and A. d'Avella, "Effective force control by muscle synergies," *Frontiers Comput. Neurosci.*, vol. 8, p. 46, Apr. 2014.
[25] A. d'Avella, A. Portone, L. Fernandez, and F. Lacquaniti, "Control of fast-reaching movements by muscle synergy combinations," *J. Neurosci.*, vol. 26, no. 30, pp. 7791–7810, Jul. 2006.
[26] A. d'Avella and F. Lacquaniti, "Control of reaching movements by muscle synergy combinations," *Frontiers Comput. Neurosci.*, vol. 7, p. 42, Feb. 2013.
[27] M. Semprini, A. V. Cuppone, I. Delis, V. Squeri, S. Panzeri, and J. Konczak, "Biofeedback signals for robotic rehabilitation: Assessment of wrist muscle activation patterns in healthy humans," *IEEE Trans. Neural Syst. Rehabil. Eng.*, vol. 25, no. 7, pp. 883–892, Jul. 2016.
[28] D. J. Clark, L. H. Ting, F. E. Zajac, R. R. Neptune, and S. A. Kautz, "Merging of healthy motor modules predicts reduced locomotor performance and muscle coordination complexity post-stroke," *J. Neurophysiol.*, vol. 103, no. 2, pp. 844–857, Feb. 2010.
[29] G. Cappellini, Y. P. Ivanenko, R. E. Poppele, and F. Lacquaniti, "Motor patterns in human walking and running," *J. Neurophysiol.*, vol. 95, no. 6, pp. 3426–3437, Jun. 2006.
[30] J. Roh, W. Z. Rymer, and R. F. Beer, "Robustness of muscle synergies underlying three-dimensional force generation at the hand in healthy humans," *J. Neurophysiol.*, vol. 107, no. 8, pp. 2123–2142, Apr. 2012.
[31] J. Roh, W. Z. Rymer, and R. F. Beer, "Evidence for altered upper extremity muscle synergies in chronic stroke survivors with mild and moderate impairment," *Frontiers Hum. Neurosci.*, vol. 9, p. 6, Feb. 2015.
[32] I. Delis, B. Berret, T. Pozzo, and S. Panzeri, "A methodology for assessing the effect of correlations among muscle synergy activations on task-discriminating information," *Frontiers Comput. Neurosci.*, vol. 7, p. 54, May 2013.
[33] H. J. Hermens *et al.*, "European recommendations for surface electromyography," *Roessingh Res. Develop.*, vol. 8, no. 2, pp. 13–54, 1999.
[34] H. J. Hislop, J. Montgomery, B. Connelly, and L. Daniels, *Muscle Testing, Techniques of Manual Examination*, 6th ed. Philadelphia, PA, USA: Saunders, 2002.
[35] D. D. Lee and H. S. Seung, "Learning the parts of objects by non-negative matrix factorization," *Nature*, vol. 401, no. 6755, pp. 788–791, 1999.
[36] J. Roh, W. Z. Rymer, E. J. Perreault, S. B. Yoo, and R. F. Beer, "Alterations in upper limb muscle synergy structure in chronic stroke survivors," *J. Neurophysiol.*, vol. 109, no. 3, pp. 768–781, 2013.
[37] J. Fagard, E. Spelke, and C. von Hofsten, "Reaching and grasping a moving object in 6-, 8-, and 10-month-old infants: Laterality and performance," *Infant Behav. Develop.*, vol. 32, no. 2, pp. 137–146, 2009.
[38] R. Melillo and G. Leisman *Neurobiological Disorders of Childhood: An Evolutionary Approach*. New York, NY, USA: Springer, 2009.
[39] J. L. Bradshaw, J. A. Spataro, M. Harris, N. C. Nettleton, and J. Bradshaw, "Crossing the midline by four to eight year old children," *Neuropsychologia*, vol. 26, no. 2, pp. 221–235, 1988.
[40] P. J. Bryden and E. A. Roy, "Preferential reaching across regions of hemispace in adults and children," *Develop. Psychobiol.*, vol. 48, no. 2, pp. 121–132, 2006.
[41] M. Rezaee, M. Shojaei, A. Ghasemi, and A. A. A. Moghadam, "What factors affect midline crossing in adult: Combined effect of task complexity and object location," *Int. J. Sports Sci. Eng.*, vol. 4, no. 4, pp. 251–256, 2010.
[42] S. Muceli, A. T. Boye, A. d'Avella, and D. Farina, "Identifying representative synergy matrices for describing muscular activation patterns during multidirectional reaching in the horizontal plane," *J. Neurophysiol.*, vol. 103, no. 3, pp. 1532–1542, Mar. 2010.
[43] I. Delis, B. Berret, T. Pozzo, and S. Panzeri, "Quantitative evaluation of muscle synergy models: A single-trial task decoding approach," *Frontiers Comput. Neurosci.*, vol. 7, p. 8, Feb. 2013.
[44] T. Afzal, G. White, A. B. Wright, and K. Iqbal, "Locomotion mode identification for lower limbs using neuromuscular and joint kinematic signals," in *Proc. 36th Annu. Int. Conf. IEEE Eng. Med. Biol. Soc. (EMBC)*, Aug. 2014, pp. 4071–4074.
[45] T. Afzal, K. Iqbal, G. White, and A. B. Wright, "Task discrimination for non-weight-bearing movements using muscle synergies," in *Proc. 37th Annu. Int. Conf. IEEE Eng. Med. Biol. Soc. (EMBC)*, Aug. 2015, pp. 478–481.
[46] T. Afzal, K. Iqbal, G. White, and A. B. Wright, "A method for locomotion mode identification using muscle synergies," *IEEE Trans. Neural Syst. Rehabil. Eng.*, vol. 25, no. 6, pp. 608–617, Jun. 2017.
[47] G. Rasool, K. Iqbal, N. Bouaynaya, and G. White, "Real-time task discrimination for myoelectric control employing task-specific muscle synergies," *IEEE Trans. Neural Syst. Rehabil. Eng.*, vol. 24, no. 1, pp. 98–108, Jan. 2016.

Sharon Israely was born in Israel, in 1974. He received the B.PT. degree in physical therapy from the University of Haifa in 2004 and the M.Sc. degree in physical therapy from Tel-Aviv University in 2011. He is currently pursuing the Ph.D. degree in the field of motor control and rehabilitation sciences with the University of Haifa.

Gerry Leisman received the Ph.D. degree in neuroscience and biomedical engineering from Union University in 1979. He held the position of a Professor of rehabilitation sciences at Leeds Metropolitan University, U.K., and concurrently at the University of Haifa, Israel. He is currently an Israeli Neuroscientist educated in Europe and the United States in medicine, neuroscience, and biomedical engineering with Manchester University. He is also the Director of the National Institute for Brain and Rehabilitation Sciences, Nazareth, Israel, a Full Professor of neuro and rehabilitation sciences with the School of Health Science, University of Haifa, and a Professor of neurology with the Department of Clinical Electrophysiology, Institute for Neurology and Neurosurgery, Universidad de Ciencias Médicas de la Habana Facultad 'Manuel Fajardo' Havana, Cuba. He is the Editor-in-Chief of the journal *Functional Neurology, Rehabilitation, and Ergonomics*.

He has been active since the early 1970s in the promotion of consciousness as a scientifically tractable problem, and has been particularly influential in arguing that a fundamental understanding of consciousness can be approached using the modern tools of neurobiology and understood by mechanisms of theoretical physics, having developed biomedical applications of continuum theory. He has also been influential in examining mechanisms of self-organizing systems in the brain and nervous system applied to cognitive functions exemplified by his work in memory, kinesiology, optimization, consciousness, death, and autism. He has likewise applied optimization strategies to movement and gait, cognition, and coma recovery. It is in this context that he, in the early 1970's, was one of the first to identify functional disconnectivities in the brain and nervous system. He was elected as a fellow of the Association for Psychological Science in 1990, a Senior Member of the Engineering in Medicine and Biology Society of the IEEE in 1986, and a Life Fellow of the International Association of Functional Neurology and Rehabilitation in 2010, having received its Lifetime Achievement Award in 2011.

Chay Machluf was born in Jerusalem, Israel, in 1989. He is currently pursuing the B.Sc. degree with the Faculty of Electrical Engineering, Technion Institute of Technology, Haifa, Israel. In his final project, he developed algorithms for processing EMG signals at the Signal and Image Processing Laboratory.

Tal Shnitzer received the B.Sc. degree (*summa cum laude*) in electrical engineering and biomedical engineering from the Technion–Israel Institute of Technology, Haifa, Israel, in 2013, where she is currently pursuing the Ph.D. degree in electrical engineering. From 2012 to 2013, she was involved in the field of signal processing and algorithms with the Israeli defense industry. Since 2014, she has been a Teaching Assistance with the Viterbi Faculty of Electrical Engineering, Technion–Israel Institute of Technology. Her main areas of interest include signal processing, biomedical signals, and geometric methods for time series analysis.

Eli Carmeli was born in Haifa, Israel, in 1955. He received the License Diploma in physical therapy from the Wingate Institute in 1980, the B.PT. degree in physical therapy from Tel Aviv University in 1987, and the Ph.D. degree from the Technion–Israel Institute of Technology in 1993. He performed post-doctoral research at the University of Florida in Gainesville, USA. He is currently an Associate Professor and a Chairperson of the Physical Therapy Department, University of Haifa. His publications and research interests investigate the aging process both on the cellular and clinical level, physical activity with individuals with intellectual and developmental disabilities and movement and public health.